Master WAVES

(Waves, Acoustics, Vibrations, Engineering and Sound)

Laser Ultrasound & Laser Indused Breakdown Spectroscopy for Non-destructive Evaluation of Wire Arc Additive Manufacturing

Master Thesis

Author : Dmitry Solodov

Tutor : Dr. Hubert Norbert

Erasmus Supervisor: Dr. Victor Espinosa

Place, date : RECENDT GmbH, Linz, Austria

Table of contents

Acknowledgements

I am deeply grateful to my advisor, Dr. Huber Norbert for his steady support and guidance throughout my master's program. His expertise and patience has been invaluable to me and have played a crucial role in the success of this thesis.

I would also like to thank Dipl.-Ing. Reitinger Bernhard and Dr. Hettich Mike for serving on my thesis committee and providing valuable feedback and suggestions. Their insights and guidance were instrumental in helping me to shape my research and write this thesis.

I am grateful to RECENDT GmbH for providing me with the opportunity to conduct my research and for all of the resources and support they provided. I would like to extend a special thanks to Dr. Edgar Scherleitner, who went above and beyond to help me with my work.

This work was done in the project "We3D" (FFG Nr. 886184) in the framework of the 8th COMET call funded by the ministry of "Climate Action, Environment, Energy, Mobility, Innovation and Technology" (BMK), the ministry of "Digital and Economic Affairs" (BMDW), the Austrian Funding Agency (FFG), as well as the four federal funding agencies Amt der Oberösterreichischen Landesregierung; Steirische Wirtschaftsförderungsgesellschaft m.b.H.; Amt der Niederösterreichischen Landesregierung; Wirtschaftsagentur Wien. Ein Fonds der Stadt Wien.

Further thanks the industry partners for their financial contributions as well as their research contributions.

Abstract

Additive manufacturing (AM) is an advanced fabrication process based on the sequential layering of materials, which is driving a transformative shift in modern manufacturing by creation of the components with enhanced geometrical complexity, reduced material waste, and improved structural integrity. AM of metal components, specifically using Wire Arc Additive Manufacturing (WAAM), involves heating of the metal to its melting point, leading to alterations in the material's chemical structure and creation of structural defects. Consequently, Non-Destructive Testing (NDT) for these materials requires both chemical analysis and physical evaluation through new non-traditional NDT techniques. This master's thesis investigates the suitability and precision of Laser-Induced Breakdown Spectroscopy (LIBS) for monitoring chemical defects in the produced material, while Laser Ultrasound (LUS) is employed to examine structural defects. The research aims at exploring the applicability and accuracy of LIBS and LUS as complementary approaches in the NDE of metallic samples. This thesis comprises four chapters, each addressing different aspects of the experimental methodology for NDE of metal components produced by the WAAM technique.

The first chapter presents some traditional NDE methods for detecting mechanical defects in metal components. In the second chapter, a more detailed description of LUS and LIBS techniques is provided, outlining their key elements and principles of operation. Chapter 3 offers an assessment of the current state of LUS and LIBS methods and showcases their application and effectiveness in evaluating AM metal structures. The experimental setup used for conducting the research and the main results obtained from the application of LUS and LIBS are further discussed in Chapter 4. Both B- and C-LUS scans are used to examine the transition from the substrate to the welded specimen, critically determining the quality of fusion between them and detecting mechanical defects. Furthermore, LIBS is employed to study model samples with varying silicon (Si) and magnesium (Mg) content, accurately determining changes in chemical composition, whether gradual or abrupt. A developed Python code facilitates visualization and processing of the acquired LIBS data. For a comprehensive NDE approach, a special aluminum sample is used to combine LIBS and LUS techniques in detecting both chemical inclusions and structural defects. LIBS is proved to be effective in identifying chemical inclusions (Mg), while LUS not only detects mechanical defects but also reveals the presence of chemical inclusions due to the density disparity and some velocity between magnesium and aluminum. The synergistic utilization of both methods demonstrates their complementarity, enabling a comprehensive NDT of the WAAM components.

1. Introduction: Non-destructive testing and additive manufacturing

1.1 Non-destructive testing

Non-destructive testing (NDT) is a set of techniques used to evaluate the integrity, properties, and quality of materials, components, structures, and products without causing damage or altering their original state. To detect weaknesses, defects, and irregularities to ensure safety, reliability and performance of critical equipment, NDT is used in different sectors. It plays a key role in quality control, maintenance and safety assurance processes.

The primary objective of non-destructive testing is to identify potential issues and weaknesses in materials or structures, allowing for timely corrective actions to be taken. The NDT method enables engineers and technicians to evaluate the condition of an object or material without having to use destructive methods that can be expensive and are time consuming. The NDT also helps to extend the life of parts and structures, reduce damage to equipment or minimize risks for failure or accidents.

Industries such as aeronautics [1], automotive [2], manufacturing [3], oil & gas[4], construction, energy [5] and healthcare use NDT to a large extent. This ensures the quality of raw materials, production products, infrastructure and different assets that are essential for a modern society. NDT plays an essential role in many industrial sectors, which helps to guarantee safety, reliability and cost efficiency while prolonging the life of assets and components due to its extensive range of methods and applications. In view of advances in technology, NDT has continued to evolve and provide even more advanced and precise testing techniques for the benefit of society and industry.

1.2 Additive manufacturing

Additive manufacturing (AM), also referred as 3D printing, is a new manufacturing technology that permits the layering of material to create three-dimensional items. In contrast to traditional subtractive manufacturing processes, which require removing material from a solid block, AM constructs items by precisely depositing material based on a digital model. This technology has received a lot of attention and has the potential to change several industrial sectors.

One of the most notable benefits of AM is its capacity to build very complicated geometries that would be difficult or impossible to achieve using traditional production processes. It makes it simple to elaborate interior structures, lattices, and hollow sections. This design flexibility provides

new avenues for product innovation and optimization in the areas including aerospace, automotive, healthcare, and consumer products.

Another advantage of AM is the ability to produce prototypes quickly. Design iterations may be implemented and evaluated fast, saving time and money over traditional prototyping approaches. AM allows for a more agile product development process, which promotes innovation and reduces time to market. AM, in addition to quick prototyping, is increasingly being utilized for end-use part production. The technology has advanced to the point that it can generate useful, long-lasting, and high-quality components for use in a variety of applications.

Furthermore, AM enables customised and unique production. With the potential to develop unique designs and tailor-made items, AM can better satisfy the demands of specific customers. This personalization extends to medical applications, where patient-specific implants, prosthetics, and anatomical models may be created, resulting in better patient outcomes and healthcare efficiency.

Although 3D printing offers a number of advantages, there are specific issues related to the quality and integrity of printed components. In order to tackle these challenges and guarantee the integrity and safety of 3D printed samples, NDT techniques are essential.

Various factors, such as materials impurities, process parameters or design mistakes, might cause defects and inconsistencies in print samples made by 3D printing processes. NDT methods can identify defects like voids, cracks, delaminations and porosity, enabling manufacturers to assess the quality of 3D printed parts and ensure they meet the required specifications. NDT can be used by manufacturers to diagnose defects that cannot be visible and assist them in identifying issues which could risk the performance of printed parts. NDT is also valuable for monitoring the health and condition of 3D printed components during their service life. Periodic inspections can detect signs of deterioration or wear which allow maintenance and minimise the risk of an unexpected failure.

In the context of the latest industrial revolution, Industry 4.0, there is a growing emphasis on integrating intelligent production systems and advanced information technologies. AM is acknowledged as a vital component of this transformative movement. The thesis offers an extensive review encompassing AM technologies, recent strides in material science, process evolution, and design considerations. The primary objective is to systematically categorize present knowledge and technological trajectories in AM, while underscoring its multifaceted utility within the Industry 4.0 landscape [6].

In this study, the NDT approaches, like LIBS and LUS are studied in application to comprehensive optical and acoustical NDT of AM. To further enhance the understanding of quality monitoring in WAAM, this work will also introduce some other acoustic techniques mentioned in the overview article [7].

1.3 Overview of the NDT methods for additive manufacturing control

Currently, a wide variety of different “traditional” non-destructive methods are used to investigate defects and control finished AM products produced by the WAAM method.

1.3.1 Ultrasound testing (UT)

Ultrasound Testing (UT) is a widely used NDT method in the context of WAAM to inspect and control the quality of produced parts. A classical UT is based on the excitation and propagation of high frequency sound waves through a material. When ultrasonic waves encounter interfaces or defects within the material, some part of the wave is reflected back to the exciting transducer (Figure 1). By analyzing the time taken for the waves to return and the amplitudes of the reflections, UT provides information about the defect severity (such as density and distribution) and location. [8]

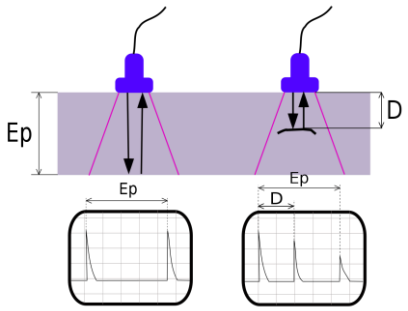

Figure 1. Defect detection by UT reflection method.

In order to detect intrinsic defects which could occur in the WAAM process, such as inclusions or holes, UT is very effective. These defects may have an impact on the properties and structural integrity of the final part. In WAAM, each successive layer is welded onto the previous one. By identifying any indication of incomplete fusion or bonding defects, UT may carry out an evaluation of the bond quality between layers. UT also makes it possible to evaluate the size, shape and orientation of defects detected, to accurately calculate and characterize them. For determining the severity and possible impact of the failure on the performance of the component, this information is essential.

1.3.2 Acoustic emission (AE)

Acoustic emission testing involves monitoring acoustic emissions, which are transient elastic waves generated by the rapid release of energy from internal changes or defects within a material.
The principle of the AE method is the following:
When a material undergoes deformation (e.g. induced by temperature gradients in the WAAM or experiences changes in its internal structure, such as the growth of cracks, dislocations, or other defects, it releases energy in the form of elastic waves. These waves can pass through the material,

and piezo-transducers are able to detect them. The piezo- transducers are converting the acoustic emission into electrical signals, which are analysed and correlated to obtain information on material properties such as position, size or magnitude of defects or changes (Figure 2).

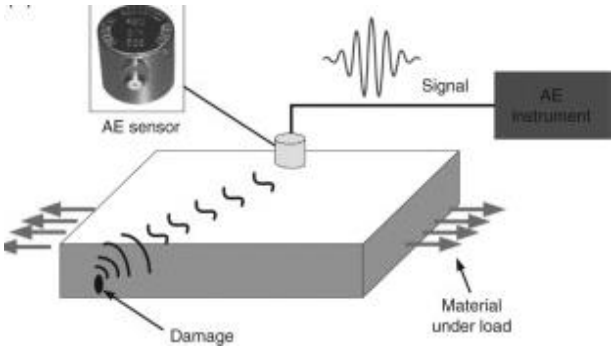

Figure 2. Schematic principle of the acoustic emission method. [9]

The AE test is well suited to detect functional defects in the WAAM components such as crack initiation, propagation, and growth. The defects may be identified without inducing damage to the part, through monitoring of acoustic emissions during or after additive production. Any anomalies of the WAAM welding process, such as lack of fusion or incomplete bonding layers, can be detected to assess the quality of the welds. [9]

1.3.3 The Electromagnetic Acoustic Method (EMAT)

The Electromagnetic Acoustic Method (EMAT) is a NDT technique that utilizes electromagnetic fields to generate and receive ultrasonic waves in metallic materials. In the material under test, EMAT generates ultrasonic waves using electromagnetic induction. The coil produces a time varying magnetic field by applying a pulsed or alternating current. The magnetic field acts upon the material, causing Lorentz forces to be generated which result in the generation of ultrasonic waves.

The range of applications of the EMAT is wide, but, in particular, this method is suited to examining the surface of WAAM metallic components. It is capable of detecting surface breaking defects such as cracks and incomplete fusion. EMAT does not require direct contact with the surface to be able to observe irregularly shaped and rough surfaces typical of WAAM, unlike conventional ultrasonic testing methods that involve a coupling agent between the transducer and the material.[10].

1.3.4. Combination of LIBS and LUS

Although all the methods above are quite effective, there is a number of serious drawbacks that make them less applicable and have an effect on the amount of information they deliver. The

combination of LIBS and LUS applied in this study offers distinct advantages for monitoring WAAM products compared to other NDT methods.

The LIBS and LUS provide complementary information about the materials both chemical composition and structural integrity, respectively. The elemental composition of the material shall be determined and quantified with LIBS by detecting impurities, inclusions or changes in metal concentration that might influence the parts properties on the surface. In contrast, LUS is capable of detecting intrinsic defects like cracks, porosity and delaminations which can give valuable information on the parts structural integrity.

LIBS and LUS can be performed remotely, making them suitable for inspecting complex geometries and hard-to-reach areas. This advantage will be of relevance for WAAM, where components may have sophisticated structures and different shapes. In order to optimise the process and ensure appropriate use of materials, LIBS is capable of identifying the special alloy or material used in WAAM. In contrast, LUS can monitor the deposition quality in order to detect problems such as incomplete fusion or bonding defect and contribute to process optimisation and quality assurance. These methods are particularly suited to ensure integrity of WAAM components and quality due to the complementary nature of these techniques; their in situ capabilities enable them to inspect a variety of shapes as well as rapid data collection. The deeper insight in the fundamentals of these techniques used in this work is presented in the next chapter.

2. Fundamentals of the LIBS & LUS methodology components

2.1 Laser fundamentals

The invention of lasers transformed a wide range of areas, from telecommunications to medicine and industry. Comprehending laser foundations is critical for understanding their applications and the underlying concepts that make them distinctive and powerful. This section examines the principles of lasers, offering insight on their functioning and potential.

The basic concepts of lasers include active media, pump source and resonator. These ingredients allow to produce a coherent, monochromatic light source with high power. Flexibility of the lasers has made them important in industries such as communications, manufacturing, medicine, and scientific research. When an excited atom or molecule is stimulated by an incoming photon of the same energy as the original excitation, it can emit a second photon that is similar in energy, phase, and direction. This stimulated emission mechanism is the foundation of laser operation and provides coherent light generation.

In order to achieve stimulated emission, a laser medium must undergo population inversion. This is the situation where there are more atoms or molecules in an excited state than in a low energy state. Usually, electrons are located in the lowest energy level known as the ground state. When an external energy source such as a light or heat is used for the atom, some electrons can rise to higher energies so that they become in excited states. However, these excited states usually last only a short time, and the electrons eventually return to the ground state, releasing the extra energy in the form of photons. When an electron in an excited state returns to the ground state, it can either release its energy spontaneously (spontaneous emission) or be stimulated by an external photon to emit a photon with the same energy, direction, and phase as the incident photon (stimulated emission).

To obtain population inversion, energy is pumped in the system through an external source of power e.g. electricity discharges, lasers and other light sources exciting a large amount of particles towards higher energy states. This process might be referred to as "inverting" an ordinary population distribution, which creates more particulate matter in excited states than in the ground state. Further amplification of the optical wave generated is achieved in a laser resonator, which consists of two mirrors placed at the ends of the gain medium. One mirror is partially reflective, allowing a fraction of the light to pass through, while the other mirror is highly reflective, reflecting most of the light back into the gain medium. The resonator enhances the intensity of the light by creating a feedback loop, causing multiple reflections and stimulating further emissions. This feedback is crucial for the amplification and generation of coherent laser light.

The optical power of a laser can also manifest in pulses of some duration at some repetition rate. Some applications (e.g. laser ablation) require the pulses having as large energy as possible at low average energy delivered to the matter. This is achieved by reducing the length of the pulses. As a result, a small volume of material at the surface of a specimen is heated in a very short time and can be evaporated.

There are various types of lasers, each with its unique characteristics and applications. Some notable examples include gas lasers (such as helium-neon and carbon dioxide lasers), solid-state lasers (such as Ti:Sa and Nd:YAG lasers), semiconductor lasers (including diode lasers), and fiber lasers. Each type has its own advantages in terms of power, efficiency, wavelength range, and pulse length making them suitable for different applications.

2.2 Laser-induced breakdown spectroscopy (LIBS)

LIBS is an advanced analytical technique that combines the power of lasers with the precision of optical spectroscopy to determine the elemental composition of materials. LIBS has gained

popularity in various scientific and industrial fields due to its almost non-destructive nature, fast analysis, and ability to detect a wide range of elements. LIBS utilizes a high-intensity laser pulse to induce breakdown and create a plasma spot, which acts as a transient light source for spectroscopic analysis. Further comparison of the spectrum obtained with the calibration curve measured for the reference material with a known composition of the elements relates the intensity of the spectral lines to the concentration of the elements (the scheme of the set up is shown on the Figure 3).

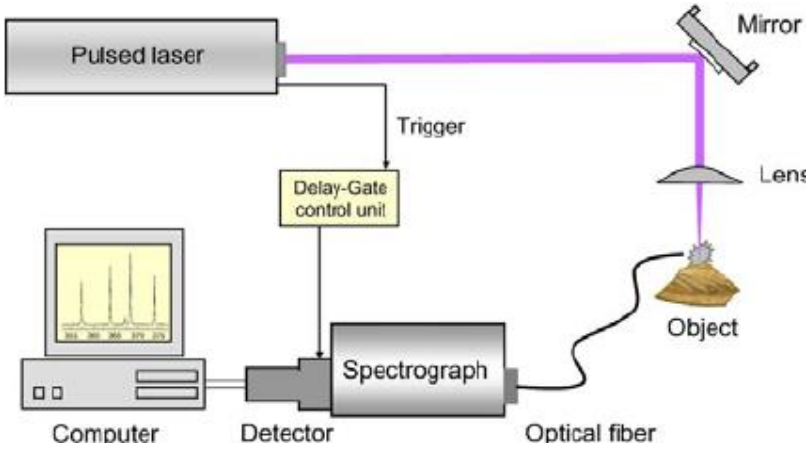

Figure 3. Typical LIBS set up

2.2.1 Plasma creation

The creation of plasma in LIBS is a crucial step that enables the analysis of elemental composition in materials. The first step in plasma creation is laser ablation. A high-energy laser pulse is focused onto the surface of the sample material. As the laser pulse interacts with the sample, the material rapidly vaporizes, transforming from a solid or liquid state into a gas. The intense energy of the laser causes the atoms within the material to lose electrons, leading to ionization. The result is the creation of the plasma composed of excited atoms and free electrons.

Due to high temperatures and pressures produced by laser ablation, plasma is rapidly expanding once it has formed. The increase in plasma is a consequence of energy and speed being released into the system that facilitates the emission of light by excited states.

2.2.2 LIBS spectroscopy

After the plasma is created there are several steps that are taking place to acquire emitted light: Within the plasma plume, the excited atoms and ions undergo transitions to lower energy states, emitting photons. These emitted photons carry information about the elemental composition of the sample material that consists of characteristic spectral lines, unique to the elements in the sample.

The emitted light from the plasma plume is collected then by optical components, such as lenses or fiber optics. These components are designed to efficiently gather and transmit the emitted

light to an optical spectrometer, which separates the light into its constituent wavelengths. The spectrometer uses optical elements such as diffraction gratings or prisms to disperse the light and provide wavelength-dependent information in a form of a spectrum. The spectrum represents the intensity of light at different wavelengths, forming a characteristic pattern of peaks and valleys.

The spectrum obtained in the spectrometer is compared to the known reference spectra to identify the elemental composition of the sample. Calibration curves can be used to establish the relationship between the intensity of spectral lines and the concentration of elements. This allows for quantitative analysis, enabling the determination of elemental concentrations in the sample.

Because of the complexity of the interaction between light and matter, the spatial and temporal distribution of laser-induced plasma is uneven [11]. The temperature of the plasma is greater in the center, while it is lower on the perimeter, which contains a significant number of low energy particles [12]. When the plasma recruits photons, these can be again absorbed by low-level particles on the periphery, causing the measured line profile to distort and the line intensity to diminish, which is known as the self-absorption effect [13]. The presence of the self-absorption effect significantly interferes with the emission spectra of laser-induced plasma and destroys the linear map, deteriorating the accuracy of LIBS quantitative analysis [14]. There are multiple existing methods to reduce self-absorption in LIBS [15-19], however, all of these methods need complicated calculations.

2.3 Laser ultrasound (LUS)

The principle of LUS is based on the generation of ultrasonic waves by laser stimulated thermoelastic expansion or ablation. This procedure begins with a laser pulse aiming at the surface of the material to be inspected (Figure 4). The material is absorbing the laser energy, which depending on the laser pulse energy leads either to localized heat and rapid expansion or ablation of the surface. These mechanisms provide two main methods of excitation of ultrasound in materials using LUS. The first type of generation is based on thermoelastic mechanism and the second one is based on ablation, i.e. evaporation of a part of the material from its surface and creating the ultrasound signal due to the conservation of momentum. The first of these methods is well studied and is a completely non-destructive method, and the second (ablation), despite the fact that some models have been already created [20-21], has not yet been fully studied.

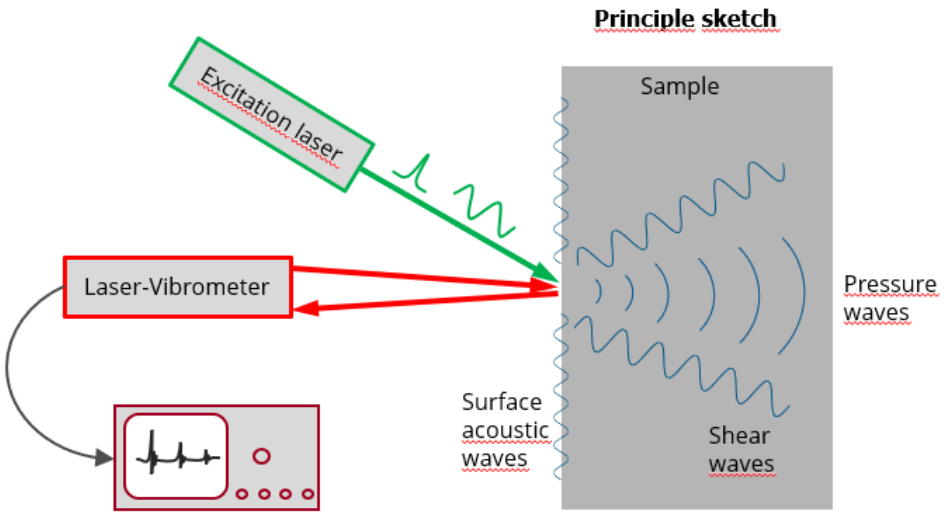

Figure 4. Scheme of the typical LUS set up

2.3.1 Thermoelastic generation

Laser pulses delivered to the material under study are typically short, ranging from nanoseconds to femtoseconds, and have high peak power. As the material heats up, it undergoes a rapid expansion, followed by thermal diffusion as it cools down. This rapid expansion create mechanical stress waves, which propagate as ultrasonic waves within the material (Figure 5). These ultrasonic waves can travel through the material and interact with internal structures, defects, or interfaces, providing valuable information about the material's integrity and properties. The choice of pulse duration depends on the desired frequency range: shorter laser pulses can produce higher frequency ultrasound waves, while longer pulses can result in lower frequency waves.

Laser- based excitation of acoustic [7] waves in the thermoelastic regime has shown promising results [21–24]. Before evaporation starts, the amplitude of sonic waves created by the laser increases linearly with pulse energy [25]. To ensure thermoelastic wave generation without harming the material, the energy and the laser wavelength must be precisely adjusted. To successfully convert laser energy into heat energy and induce thermoelastic expansion, the material should be idealy very absorbent to the laser light.

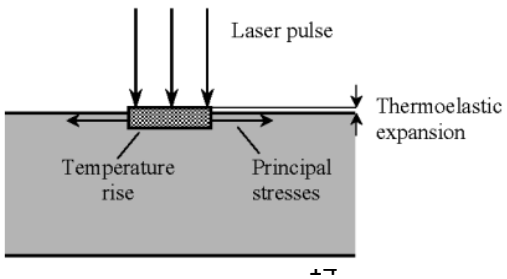

Figure 5. Thermoelastic LUS generation [26].

2.3.2 Ablation generation mechanism

In contrast, the ablative regime avoids such interference issues because it induces mechanical waves directly through rapid vaporization or ablation of the material's surface. In the ablative regime the surface begins to melt and subsequently vaporizes. The melt front begins to spread from the surface into the substance. Continued heating gets the substance to the point of vaporization. At this time, the matter is expelled from the surface, and the vapor as well as surrounding air are ionized as a result of numerous physical processes, forming a plasma plume that extends away from the laser spot on the surface. The impact of the extended plasma plume onto the surface of the specimen leads to a strong reactive force that generates an acoustic wave pulse (Figure 6, b [7]).

Understanding of the laser acoustic wave creation in the ablative domain is critical for various reasons. There are several ultrasonic inspection applications in which little surface damage can be tolerated. To take advantage of the substantial acoustic wave enhancement achievable in the ablative domain, it is critical to have a clear grasp of the vaporization process in these instances. This may enable the creation of high-amplitude acoustic sounds while remaining under a certain damage tolerance threshold [27]. If the link between ablative acoustic signals and surface damage [28] is clearly defined, the acoustic signature may be employed for both process inspection and surface damage monitoring at the same time [25]. Figure 4 summarizes a typical scheme of the two diverse ultrasound wave excitation mechanisms: thermoelastic and ablative.

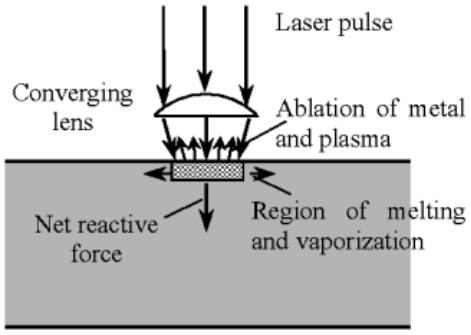

Figure 6. Ablative mechanisms in LUS [29].

2.3.3 LUS propagation and interaction with defects

Ultrasonic waves generated by laser-ultrasound excitation propagate through the material and carry valuable information about its internal structure, properties and defects. Laser-generated ultrasound

may interact with defects in a variety of ways, providing useful information on their presence, location, and features. When an ultrasonic wave hits a defect such as a crack, vacancy, or inclusion, a portion of the wave is reflected towards the source. The amount of reflection depends on the acoustic impedance mismatch between the materials involved. To detect and analyze reflected ultrasonic waves are being used to investigate the existence of abnormalities and estimate their size and form. For this purpose, three types of ultrasonic scans are most commonly used in the reflection mode (Figure 7):

- A-Scan shows the amount of acoustic energy reflected as a function of time for a single position of radiation transducer.
- B-scan is an amount of A-scans obtained for a line movement of the exciting transducer.
- C-scan is the distribution of the amplitude of the reflected ultrasonic signal as a function of 2D position on the surface of the specimen. It characterises reflected properties inside the sample (including defects) for the transducer moving along the total surface of the specimen.

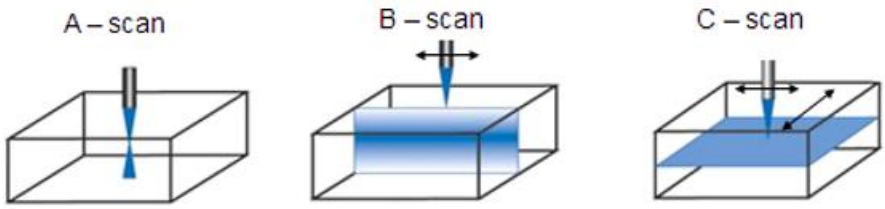

Figure 7. Types of ultrasonic scans that are being used in the reflection mode

Ultrasound waves can also be scattered by defects, causing them to shift direction and spread out in different directions. The scattering provides insight into the microstructural properties of materials and the presence of small defects and inhomogeneities.

LUS can also undergo mode conversion when interacting with defects. Mode conversion refers to the transformation of one mode of ultrasound wave (e.g., longitudinal wave) into another mode (e.g., shear wave) upon encountering a defect. These mode conversions can provide information about the elastic properties and structural characteristics of the defect and the surrounding material.

Changes in the attenuation of ultrasonic waves can also be caused by material defects. The steady reduction in the amplitude of ultrasound as it propagates through a medium is referred to as attenuation. Defects can produce extra scattering and absorption of ultrasonic waves, changing the attenuation properties.

The most obvious effect of ultrasound encounter with defects is, however, variation in the time-of-flight of ultrasound waves. It is, therefore, feasible to determine the presence and location of flaws inside a sample by monitoring the time-of-flight of LUS.

2.3.4 Detection of LUS

The LUS generated waves are detected with a special laser interferometer or acoustic transducer, to convert them into signals that can be used for analysis on material properties and possible defects. There are 2 most popular methods of LUS detection that will be discussed below.

First method is LUS detection utilizes a separate laser beam, often a continuous-wave laser, directed at the materials surface. The ultrasound waves, generated by a laser pulse, are causing transient displacements on the surface and lead to changes in the phase of the steady laser beam. These changes are measured by an interferometric scheme and provide information on the ultrasonic waves and material characteristics.

Different types of interferometers are designed for specific applications, and they vary based on the kind of waves used (such as light or sound) and the measurement they're intended for. There are several interferometers that are commonly used: Fabry-Perot, Laser Dopler, Shearing Interferometer. In this work, the Two - Wave Mixing (TWM) Interferometer was used.

Alternatively, piezoelectric transducers can be employed to detect the ultrasonic waves generated by the laser. The pressure waves that penetrate in the piezo-material induce the strain-stress inside the piezoelectric transducers. In response, this mechanical action generates an electric field and voltage across the transducer faces, i.e. the signal that provides detection of LUS.

2.4 Wire Arc Additive Manufacturing (WAAM)

Wire Arc Additive Manufacturing is a method of AM that uses an electric arc as a heat source to melt and deposit metal wire layer by layer, eventually building up a three-dimensional item.

This AM technique emerges as a promising solution to produce medium to large scale components [30]. Its advantages, including high deposition rates, an unlimited build volume, and cost-effectiveness position WAAM as a strong contender for replacing traditional methods in aerospace component manufacturing and other industries. The reductions in material waste and lead time, combined with increased design freedom, complement its appeal in various industries.

A welding power supply is utilized in the WAAM process to produce an electric arc between a metal wire electrode and the substrate. The heat from the arc melts the wire, and a motion system regulates the placement of the welding torch to deposit the molten metal along a specified path onto the targeted locations. As each layer hardens, the next layer is put on top, and so on until the entire item is completed (Fig. 8).

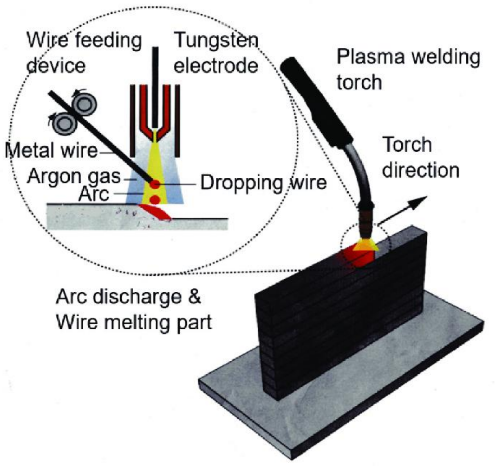

Figure 8. WAAM 3D printing method.

The wire feedstock used in WAAM is less expensive than metal powders used in other processes. This decreased material cost translates to a lower total part production cost. WAAM may also be conducted with commercially available welding equipment, making it accessible and adaptable to current welding infrastructure. WAAM's high deposition rate, obtained by using thick wire feedstock, enables creation of components with shorter times when compared to other AM technologies. As a result, WAAM is particularly suited for applications requiring the manufacturing of large and structurally complicated components, such as those in the aerospace, automotive, and marine sectors.

However, on the other hand, this 3D printing technique has certain restrictions. Because of the large diameter of the wire feedstock, the technique is better suited to manufacturing bigger, thicker components rather than small and delicate geometries. Surface polishing may also be necessary for some applications since WAAM produces a coarser surface than other AM processes.

Despite its potential, the lack of a commercially available platform currently limits its industrial evaluation and adoption. However, ongoing efforts to develop manufacturing software capable of producing parts automatically are paving the way for wider integration of WAAM in existing manufacturing processes.

The review of recent technological developments in WAAM highlights its potential as a versatile and promising process for producing high-quality components [31]. The focus on microstructure, mechanical properties, process defects, and post-process treatment emphasizes the need for a quality-based framework to ensure defect-free and reliable fabrication.

3. WAAM NDT via LIBS&LUS: State-of-the-art

NDT of the WAAM metallic components by using LIBS&LUS manifests a series of crucial benefits compared with traditional techniques (e.g. remoteness and in-situ operation). However, their application in WAAM NDT has started only in recent years and is in inception stage described below.

3.1 WAAM NDT with LIBS

In recent years, the LIBS capabilities in non-destructive and rapid chemical analysis have attracted considerable attention. The state of LIBS technology and the most recent developments will be the subject in this part.

One of the primary benefits of LIBS is that it is non-contact and non-destructive. The approach involves little sample preparation and may be used on a wide range of materials, including solids, liquids, gases, and even biological samples. Another LIBS benefit is that it can examine materials in real time, in situ. The possibility of LIBS in situ measurements are shown in a recent paper [32], where the researchers have introduced a cutting-edge technique that showcases the potential of LIBS for in-situ quantitative multi-elemental analysis during the additive manufacturing process. A compact LIBS probe was designed and integrated into the laser cladding head, enabling the real-time assessment of essential components during the synthesis of high wear-resistant coatings. Both the hot solidified clad and the melt pool surface were tested, with superior analytical results observed.

Another study explores the use of LIBS during Tungsten Inert Gas (TIG) welding of stainless steel [33]. The research successfully demonstrates the feasibility of in-situ quantitative multi-elemental analysis at a predetermined location behind the welding torch. By employing algorithmic filtering techniques, the researchers achieve accurate chemical composition measurements, particularly for Chromium (Cr), Nickel (Ni), and Manganese (Mn) elements. The study presents potential solutions to reduce background effects caused by the weld plume, paving the way for improved real-time quality control during welding processes.

A comparison with other established analytical techniques reveals that while some methods may be more sensitive and accurate, LIBS possesses unique features that make it appealing for chemical elemental analysis. The technique's distinctive capabilities, such as no sample preparation, remote detection, and compact instrumentation, contribute to its attractiveness [34]. With continued development of the method and instruments,LIBS is able to become the most appropriate analytical technique for qualitative and quantitative analysis of the WAAW produced metallic components.

3.3 WAAM NDT with LUS

Research in the field of LUS NDT has led to significant technological advancements. Improved laser sources, such as ultrafast and high-power lasers, have enhanced the generation of ultrasound, resulting in improved signal-to-noise ratios [35] and increased inspection speed. Additionally, advancements in optical detection and signal processing algorithms [36] have enabled higher sensitivity and better resolution, leading to more accurate defect detection and characterization.

One application area where LUS has shown exceptional promise is NDT of defects typical for AM. The technique is used to inspect complex internal geometries and detect defects, such as porosities and inclusions, which are critical to ensuring the quality and reliability of 3D-printed components. LUS has also been used in the inspection of welds, composites, and other advanced materials, where traditional NDT methods may be limited.

Yan Zeng., et. at. [37] explores the feasibility of non-contact inspection of WAAM components using LUS. The LUS, comprising a pulsed laser excitation and a laser interferometer for detection, are employed to inspect artificial defects (crack, flat bottom hole, and through hole) in a WAAM sample remotely and without surface machining.

D. Lévesque [38] shows successful application of LUS combined with the synthetic aperture focusing technique in the inspection of additive manufactured coupons of INCONEL® 718 and Ti-6Al-4V and demonstrates its potential as a valuable non-destructive testing method for quality control in the additive manufacturing industry. The detection of critical defects such as lack of bonding, lack of fusion, and discrete porosity holds significance for ensuring the integrity and reliability of additively manufactured components. Moreover, the ability to perform real-time measurements during the manufacturing process opens opportunities for on-line implementation, thereby facilitating immediate feedback and adjustment to optimize the manufacturing process.

3.4 WAAM NDT using combination of LIBS and LUS

Yuyang Ma,. et al. [39] created and used a new approach for laser opto-ultrasonic dual (LOUD) detection (in fact a combination of LIBS&LUS methods) for simultaneous and real-time detection of chemical elemental compositions, and mechanical defects , like, structural defects, and residual stress in aluminium (Al) alloy components during WAAM processes. They demonstrated the effectiveness of LOUD in obtaining Si elemental mapping, 2 mm preset defect detection, and weld residual stress distribution in a laser-welded sample simultaneously. Additional experiments using LOUD achieved Cu element mapping, 1 mm defect detection, and residual stress assessment in a WAAM sample, with consistent outcomes compared to conventional detection methods. LOUD offers the advantages of timesaving, cost-effectiveness, and non-destructiveness [39].

Metal-based AM holds immense potential in various industries, but its manufacturing quality often lacks stability, necessitating the need for component properties detection. Grain size distribution significantly influences mechanical properties in AM, while the distribution of added elements, like titanium (Ti), affects the grain size of aluminum (Al) alloys. Yuyang Ma, et al. [36] in their study, employed laser opto-ultrasonic dual (LOUD) detection to investigate grain size and element distributions in WAAM with an Al alloy. The results showed that the average grain size obtained from ultrasonic measurements matched electron backscatter diffraction results, validating LOUD's accuracy. Furthermore, optical spectra revealed Ti enrichment corresponding to grain refinement areas, which was confirmed by X-ray diffraction (XRD) spectra shifting towards AlTi and Al2Ti forms in Ti-rich regions. Therefore, the combination of the LUS & LIBS is an effective approach enabling to simultaneously analyze both mechanical and chemical properties, aiding in understanding complex physical and chemical changes in WAAM process.

4. Experimental set-up and the Results

4.1 Experimental set-up

As it is shown above, LIBS enables elemental analysis of the surface through plasma emission spectroscopy, while LUS provides non-destructive evaluation of internal structures using ultrasonic waves. Although these methods traditionally use separate setups, this thesis proposes an innovative approach to unify their capabilities into a single combined setup, driven by a common excitation laser.

The proposed integrated setup (Figure 9a) leverages the advantages of a water cooled doubled pulsed Nd:YAG laser, Quantel Q- smart (Merion MW, wavelength - 532; pulse duration- 9ns; max pulse energy – 300mJ, pulse repetition rate – 100Hz) which serves as an excitation source for both LIBS and LUS in the ablative regime. The laser beam was guided by the mirrors to the material surface and focused with a lens to generate the plasma. The plasma spectrum was gathered with a light collector fiber coupled with a spectrometer (Avantes, AvaSpec-ULS2048CL-EVO), which covers a range from 185 nm to 461 nm with a resolution of 0.4-0.6 nm. Spectrometers like the AvaSpec-ULS2048CL-EVO are intricate optical instruments that analyze and evaluate light properties. They comprise entrance optics to gather light, collimating optics to align the beams, and dispersion elements (diffraction grating or prism) to split light into diverse wavelengths. Focusing optics channel these dispersed wavelengths onto a detector array, each pixel capturing the corresponding intensity. Electronics converts signals into digital data, while software processes and calibrates this data, generating a spectral output. A python code was developed during the Master thesis to proceed and visualize this digital data that are coming from spectrometer. Meanwhile, an ultrasound signal was

received by TWN. The pulsed detection fiber laser Tecnar Lus Advance (Firing rate- 100 Hz; working power – 250W; pulse width – up to 80 µs; optical wavelength – 1064nm) is being used for lightning the surface. The laser was triggered by a software made by RECENDT GmbH using LabView coding language. By utilizing the same laser for both techniques, we eliminate the need for redundant laser systems, reducing setup complexity and costs.

a)

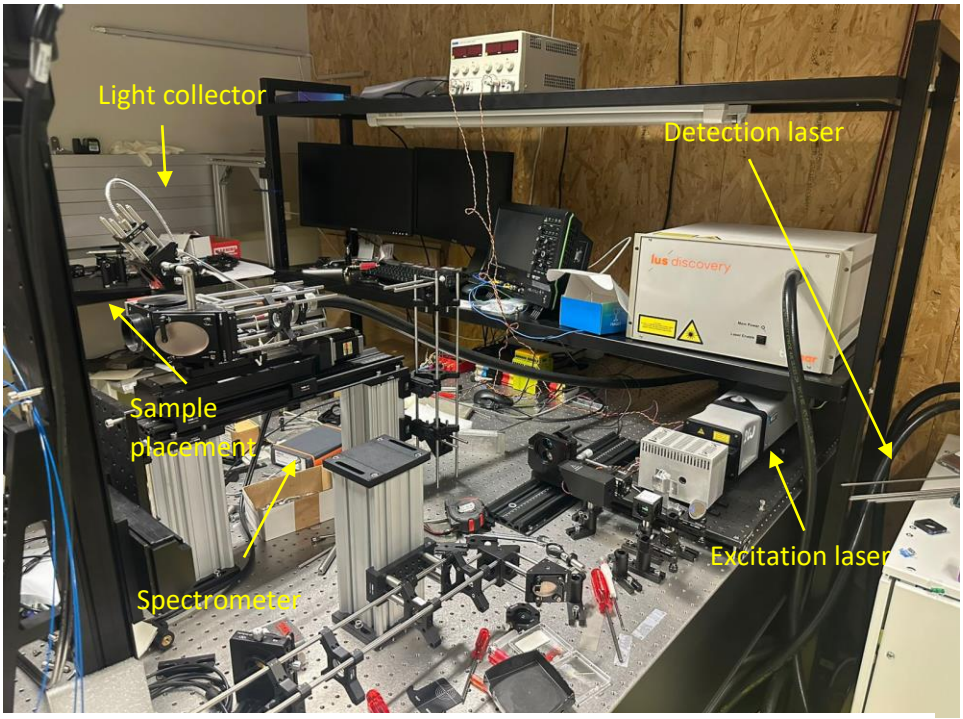

b)

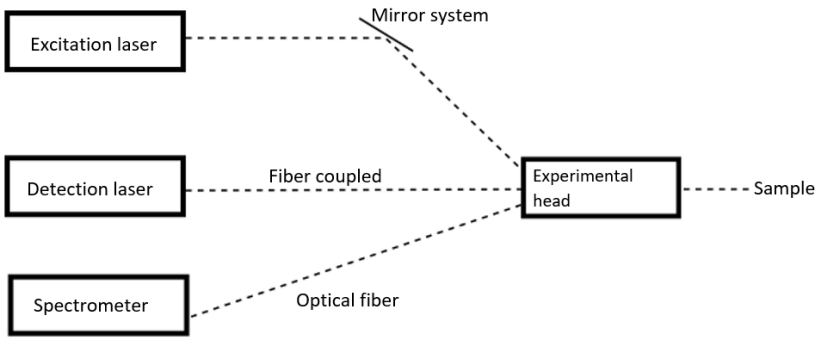

Figure 9, a,b: Laboratory set up implemented for LIBS & LUS techniques (a), Interconnection between the elements of the set up (b).

The integration of LIBS and LUS techniques offers several benefits, including enhanced material characterization, reduced measurement time, and improved detection sensitivity.

Furthermore, the simultaneous acquisition of elemental and structural information minimizes the need for multiple sample preparations and measurements, making the approach efficient and cost-effective.

4.2. Results of the measurements

4.2.1 Laser Ultrasound results

In the first part of our study, an evaluation of the AM components using LUS was implemented. We have been able to detect and analyse various subsurface defects, such as holes or other internal defects, using a pulsed laser that generates ultrasonic waves in the components. The LUS data obtained were subjected to signal processing techniques, allowing for defect visualization and characterization with high precision.

Figure 10 shows the sample of steel K 56 manufactured with the WAAM technique used for the study. The LUS excitation position and the laser scanning direction (B-scan) are shown in Fig. 8. Steel K 56 represents a relevant and widely used material in multiple industrial applications.

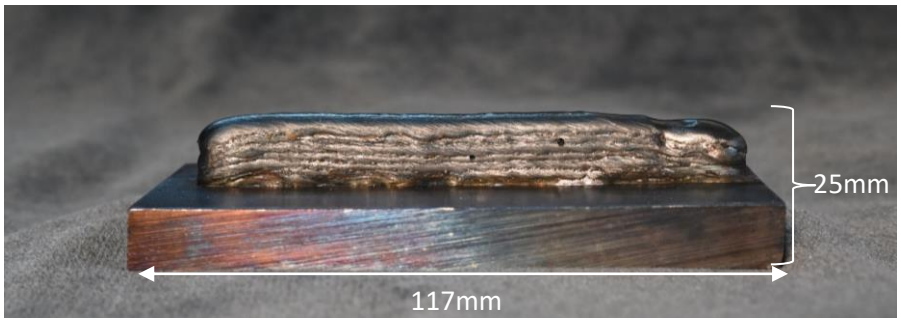

Figure 10. Optical photo of the sample on the substrate plate made by WAAM method for LUS examination (Steel K56).

The dimensions of the steel K 56 specimen manufactured using the WAAM method are also indicated in Figure 10. The LUS measurement was performed using the state-of-the-art pulsed laser system (Nd:YAG Merion MW) in the ablation regime. The laser excitation was applied successively to the top and the bottom surfaces of the steel sample, causing an ultrasonic wave to propagate through both background plate and the AM specimen. The ultrasonic signals reflected from the interface plate-specimen and the top of the specimen were captured by another (receiving) laser pointed at the same spot as the excitation one and scanned synchronously with the excitation laser, allowing for a high degree of accuracy in data acquisition.

In the first experiment, the B-scan of the Laser Ultrasonic evaluation was initiated from the bottom of the presumably intact steel K 56 sample (as shown in Figure 11) to thoroughly examine the

presence of internal defects mainly in the lower part of the component. This approach has allowed us to assess the internal structure of the WAAM produced component and to identify any potential flaws or irregularities that could affect its mechanical properties and overall quality.

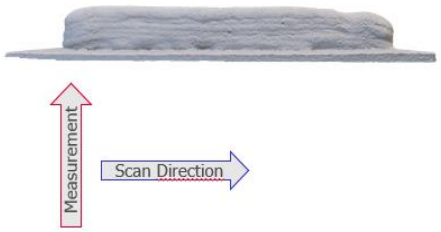

Figure 11. Bottom LUS scan of the 3D model of the K56 sample.

In order to obtain the most accurate data, and to detect the ultrasonic wave amplitude variations, precise adjustments have been made to laser parameters and ultrasound detection settings during the initial scan: the excitation energy was chosen to be 30 mJ, scanning speed – 10mm/s, distance from the scanned surface – 12cm.

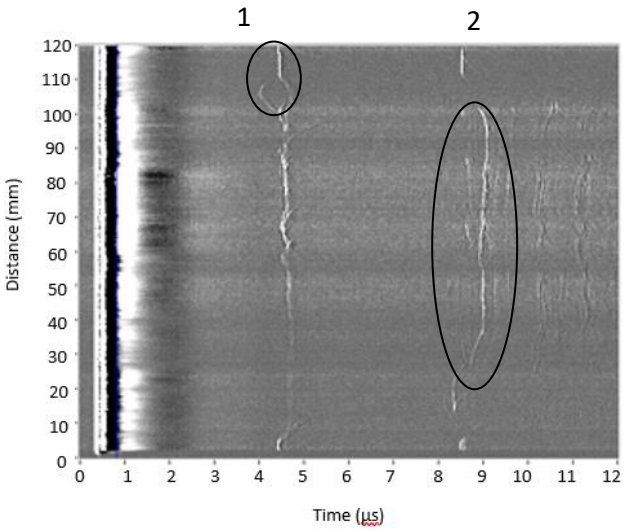

Figure 12. B-LUS scan of the steel sample from below

The B-scan results (Figure 12) indicate the two major reflections that take place in each A-scan on the way of the LUS pulse to top of the specimen (bright lines in Fig. 12): the time of flight for the first reflection corresponds to the interface between the base-plate and the specimen (marked as 1), while the second one is the back wall echo, corresponding to the top side of the specimen, is indicated by number 2.

Therefore, the lack of the reflections with a smaller time of flight (line 1) would indicate the absence of major internal defects or irregularities induced on the substrate by the first welding layer.

Such a case, can be clearly seen in Fig. 12: the reflection from the top part of the base-plate at the beginning of the scan (left hand side of the specimen in Figs. 10,11) is noticeably weaker than at the end. Additionally, the existence of a strong interface defect resembling a bubble is readily identified in the final section of the scan at around 100-110 mm. The quality and integrity of the welding line in this region confirmed by the reflected LUS B-scan is necessary to ensure overall stability of the AM operation.

The back wall echo (line 2) overall displays a clearly defined and quite consistent ultrasonic reflected pattern (Fig. 12). Nevertheless, one can notice in Fig. 12 the doubling of the reflection from the topside of the sample in the upper part of the B-scan. This finding suggests a poor bonding between some final layers of the specimen, leading to the occurrence of reflections. In the area between lines 1 and 2, no other reflection anomalies have been detected which would indicate high quality welds with no indications of defects that might occur in the WAAM process.

To obtain information on 2D-bonding layer between the AM component and the substrate the LUS C-scan has to be used. The data acquisition program (LUVIS, developed by Dr. Huber Norbert) was applied, to reconstruct the acoustical C-scan by combining multiple LUS B-scans measured. It enables to fully evaluate the quality of the initial layer of the WAAM-produced steel K 56 sample, specifically focusing on how well it had been deposited on the substrate. This initial layer is crucial for determining the overall bond strength because the entire structural stability of the AM component may be jeopardised if there are any discrepancies or defects in this layer.

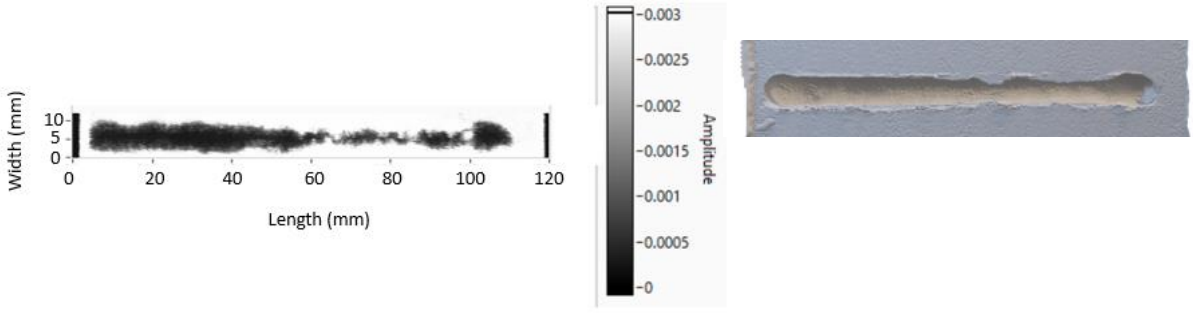

a) b)

Figure 13, a, b : LUS C-scan of initial layer (a), Optical form reconstruction of the first sample layer (b).

Figure 13a presents a C-scan image of the intermediate layer between the substrate and the specimen, acquired using laser ultrasound. Figure 10b displays the optically reconstructed initial layer, which was obtained through the 3D laser scanning of the sample. The optical image indicates

the insufficient welding quantity in the right hand side of the layer. As evident from Figure 12a, the laser ultrasound image also effectively captures the geometric contour of the transmission layer similar to the optical counterpart. Besides, a noticeable discrepancy in bonding quality becomes apparent, particularly in the right hand side part of the layer, where the amplitude of the reflected C-scan signals are higher (see the colour scale) and the weld exhibits the optical signs of poor welding as well. In contrast, the homogeneous welding in the left hand side part displays both a highly satisfactory weld with excellent bonding (low amplitude of the reflected signal, black in colour scale).

Figure 13 thus provides a convincing visual representation of the original layer and the distribution of the bonding strength in it obtained by LUS C -scan. The comparative analysis shows a high degree of similarity between the two approaches and also reveals the existence of several production errors at the initial layer. The areas with the absence of proper bonding are a cause for concern, as they could potentially compromise the structural integrity of the AM component.

In the second test of the LUS evaluation, the sample was scanned from above to assess its ability to detect artificial defects. The defects in the form of two drilled holes with a diameter of 1 mm each (see Fig. 10), were deliberately created prior to the scanning process. In steel samples produced using the WAAM process, the size of defects can vary based on several factors, including the specific WAAM setup, material properties, process parameters, and post-processing procedures. However, typical defect sizes can range from small pores or inclusions measuring a fraction of a millimeter to larger irregularities that might be a few millimeters in size [40]. The assessment of the LUS ability to reliably detect these artificial defects has been a primary objective of this test.
The drilling of holes served as a controlled method to introduce known defects into the sample. By creating the defects with a standard size and shape, we could precisely assess the LUS systems sensitivity and resolution in detecting these specific artifacts.

During the scanning, ultrasonic waves were generated by a laser pulse aiming directly onto the top surface of the sample. The scheme of this experiment is presented below in Figure 13.

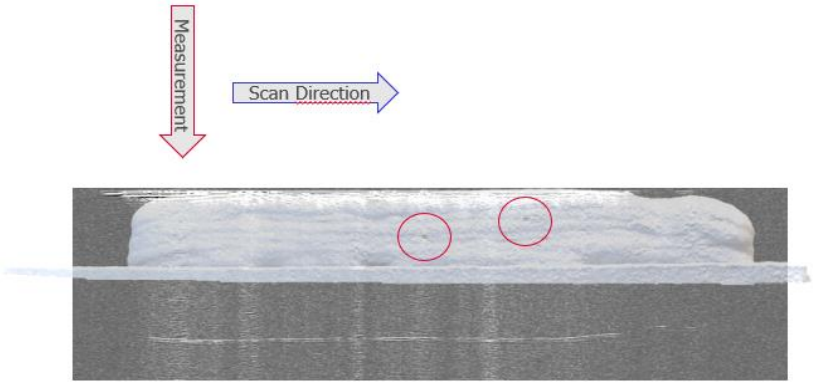

Figure 14. Second test setup. Position of holes detected by LUS overlapped with real positions of the holes in red (side view).

According to the B-scan presented In Figure 15, the LUS effectively identifies and locates both artificial defects, confirming its ability to detect minute flaws at least with a size of the order of 1 mm.

1-millimeter-diameter perforations were created to assess the capability of LUS in detecting sufficiently sizable flaws. This evaluation aims to pave the way for the potential consideration of smaller defects in future applications.

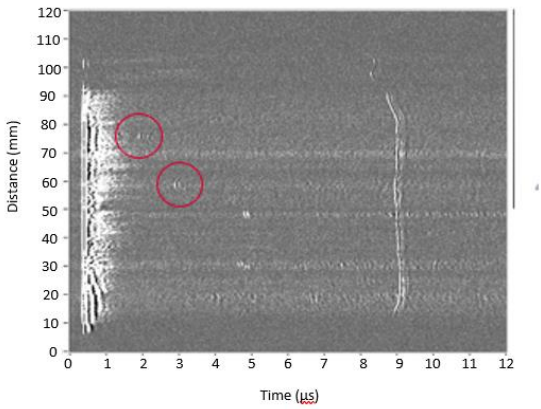

Figure 15. B-scan results of LUS detection of the artificial defects.

The fact that the laser ultrasonic technique has a accurate ability to locate the defect positions, is illustrated in Figure 15. Actually, the horizontal coordinate of each hole position can be directly read in the sequence of the B-scans in Fig. 15. The 2D-positions of the defects obtained are shown in Fig. 14 overlapped onto the positions of real holes in the optical specimen image. Coincidence provides compelling evidence that the laser ultrasonic system is accurate in its both detection and location positions of defects.

Overall, our tests prove the potential of the Laser Ultrasonic LUS system as a valuable instrument to assure quality in AM production.

4.2.2 LIBS results

4.2.2.1 NDT of Si gradient in Al

The LIBS measurement of the WAAM-produced aluminum sample (Fig. 16) was aimed to reveal a chemical composition gradient throughout its height, indicating the presence of two distinct alloys:

Al4047 at the top of the sample and Al4018 alloy in the base. This sample was produced with a two wire feeding system, thus it was possible to change the content of the alloy by reducing the amount of one alloy and increasing the amount of the other alloy. Moreover, a significant chemical gradient, particularly in the silicon (Si) component, was observed along the height of the component.

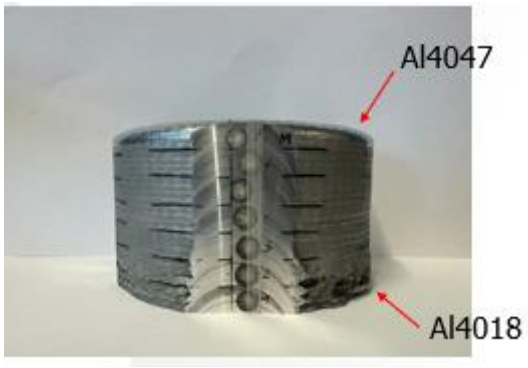

Figure 16. LIBS sample with Al alloy and Si gradient over the height.

In order to be able to analyse the chemical composition of the sample in detail, LIBS measurements of the distinctive spectral signatures have been made at various sites along the height of the sample. Chemical compositions of these two alloys are presented in the Table 1 below.

Table 1. Comparison of the chemical compositions of the two Al alloys.

Fabrication specs		
Component	AL4018	Al 4047
Fe, (%)	≤ 0.2	≤ 0.8
Si, (%)	**7**	**13**
Mn, (%)	≤ 0.1	≤ 0.15
Cu, (%)	≤ 0.05	≤ 0.3
Zn, (%)	0.1	≤ 0.2
Mg, (%)	0.5	≤ 0.1
Al, (%)	≤ 92.1	≤ 70.9

Table 1 clearly indicates that there is a significant difference in the silicon (Si) component between the two alloys, with alloy Al4047 containing approximately twice the Si content compared to Al4018. This noticeable contrast in Si concentration suggests that the LIBS method should be well-suited to distinguish and differentiate between these two alloys based on their Si composition. Figure 17 presents a comparison between the results obtained from LIBS and spark spectroscopy for the silicon gradient observed in the WAAM-produced Al sample. This Figure demonstrates how

closely the LIBS measurements trace the spark spectroscopy results, confirming its accuracy and reliability in determining the variation in silicon content along the height of the component.

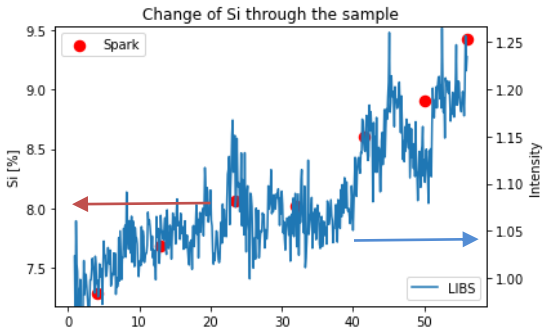

Figure 17. Change of Si content over the height of the sample.

In the measurements, we specifically focused on the Si emission line at 288 nm and normalized it with respect to the Al emission line at 265 nm within the sample using self-made Python code that allows us to plot all necessary information about chemical composition of the samples. Information about the existing spectral lines for each of the elements was obtained using NIST LIBS Database [41] It also normalizes the lines and could be suitable for plotting and tracking distribution of any element that is presented in the material. The normalization process allowed to properly evaluate the variation in Si content over the entire sample height. It is clear visible, that the results of LIBS and spark spectroscopy have a high degree of overlap: a blue irregular line representing LIBS data, closely reflects the results of spark spectroscopy marked with red dots. This close correlation between the two sets of data is consistent with LIBS and spark spectroscopy agreement on Si content determination in a sample.

However, it is worth noting that the spark spectroscopy results revealed a discrepancy in the maximum Si content achieved at the top of the specimen. The spark spectroscopy data indicated a maximum Si content of 9%), whereas literature expectations (Table 1) suggested a higher value of 13%. This deviation between the spark spectroscopy results and the theoretical Si content raises an important consideration for the materials actual properties. A number of factors, e.g. experiment limitations, sample heterogeneity and the presence of other alloying elements that might interact with Si detection, could be attributed to this discrepancy**.**

Despite this discrepancy, the overall agreement between the LIBS and spark spectroscopy results for the Si gradient indicates that both techniques effectively capture the general trend of Si content variation along the height of the sample. The LIBS ability to non-destructively and rapidly analyze elemental composition remains a valuable asset for quality assessment in AM.

4.2.2.2 Mg gradient

Three different aluminum plates have been used to study the potential of LIBS in determining magnesium (Mg) gradients in a variety of concentrations. The aluminum sheets were thoroughly prepared to have a concentration of Mg of 1.2%, 3% and 5% (Figure 18). The arrangement of the plates from left to right had an ascending magnesium content order, with the left plate containing 1.2% Mg, the middle plate consisting of 3% Mg and the right plate with 5% Mg.

In the LIBS measurements, the laser was focused on the surface of each aluminum plate, generating plasma which emitted characteristic spectral lines. The spectral lines were similar to that of the constituents detected in the samples, e.g. magnesium. Based on the analysis of the wavelength lines LIBS complemented with the code developed was used for the quantification and assessment of Mg concentration gradients. This analysis is particularly significant in the context of additive manufacturing and material development, as Mg-aluminum alloys are widely used in various industries due to their desirable mechanical properties, lightweight nature, and corrosion resistance.

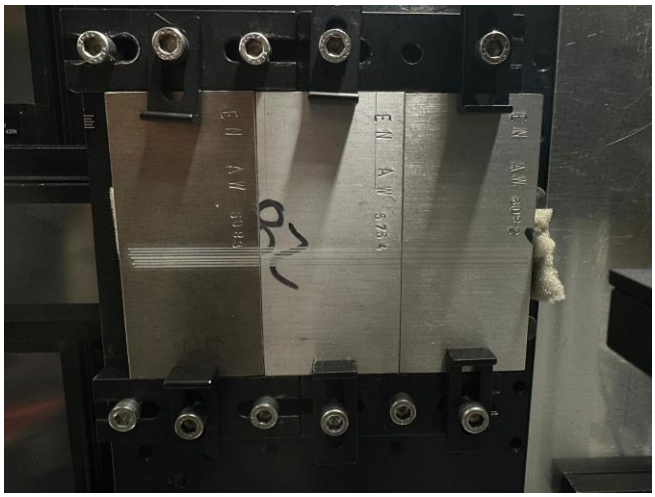

Figure 18. Al plates samples with different Mg content.

The results of the LIBS experiment are displayed in Figure 19, revealing a prominent and sharp increase in magnesium (Mg %) content each time the laser reaches the next plate with a higher Mg concentration. To demonstrate these results Mg line 383 nm was normalized in respect to the Al emission line at 265 nm within the sample using self-made Python code. The LIBS measurement was made in the direction from right to left on the Figure 18. The plot illustrates a clear and distinct stepwise pattern, with each step corresponding to the transition from one plate to the next with an increasing Mg percentage.

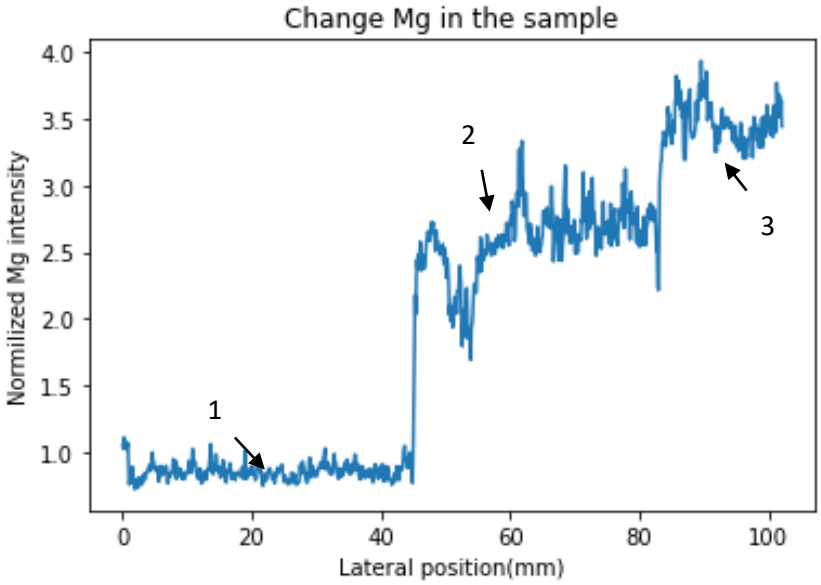

Figure 19. Change of Mg component in three Al plates.

Due to the lack of the reference specimen, the results presented in Figure 19 do not directly show the exact Mg percentage in each plate. Instead, the plot displays the change in intensities of the spectral lines specific to magnesium as the laser interacts with the different plates. Three numbers (1,2,3) are displayed, each representing different levels of intensities of Mg spectral line for three distinct aluminum plates: AW5083, AW5754, and AW6082.

The results presented demonstrate the capability of the LIBS technique to detect and register changes in chemical composition, specifically the variations in Mg component in aluminum plates. While the exact values of Mg percentage are not explicitly provided, the changes in spectral line intensities are indicative of the relative differences in Mg content among the samples. The ratio of the intensities of Mg lines and the proportion of the Mg content in samples were calculated. The ratios of intensities and magnesium content are highly similar with 1.3 and 2.5 in the Mg observed by LIBS and 1.5 and 2.5 respectively with a real percentage of Mg in the aluminum alloys.

The consistent proportionality between the intensity changes and the expected Mg percentage provides a strong evidence of the reliability and accuracy of the LIBS technique for qualitative Mg

Controlling the Mg component in the WAAM alloys holds critical significance due to its profound impact on the material's performance and properties. The Mg content plays an essential role in shaping the mechanical characteristics of this alloy, such as its corrosion resistance, microstructure and weldability. The mechanical properties of the WAAM alloy, such as strength, ductility, and hardness, are directly influenced by the Mg content [42]. Additionally, Mg content plays a crucial role in determining the alloy's weldability. High Mg concentrations can lead to welding-related issues, making it necessary to carefully control the Mg content to ensure proper weldability and facilitate the manufacturing process.

4.2.3 LIBS and LUS methods combined

The final sample under investigation was an aluminum specimen fabricated using the WAAM method, incorporating magnesium inclusions by fusing magnesium rods into the sample (chemical defects) and a pair of drilled holes (artificial mechanical defects). The sample was designed with two welded aluminum walls on an aluminum substrate, as illustrated in Figure 20. In order to obtain information on the defects both LIBS and LUS were supposed to be used in this study.

a) b)

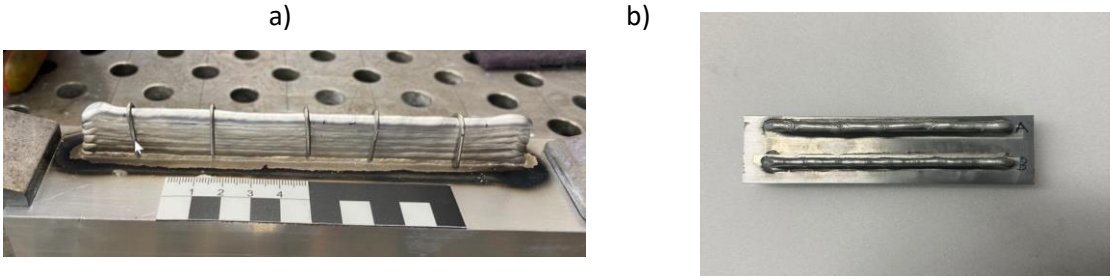

Figure 20. Top-view (b) and side-view during production(a) of the aluminum specimen with Mg rods infused.

LIBS was employed to assess the Mg component in the sample. During the LIBS scan, the laser beam was directed onto the top of the sample's surface. The aims of LIBS were two-fold: first, to detect any changes in the Mg component throughout the scan and, second, to accurately identify the positions of the fused Mg rods (5 rods were welded into the sample).

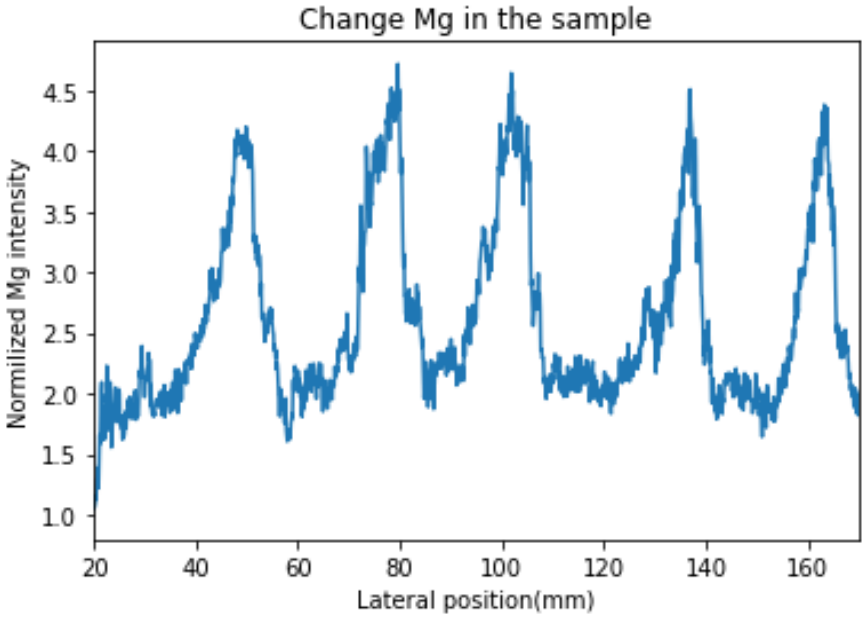

Figure 21. Change of Mg in aluminum sample through the surface scan

Each peak displayed in Figure 21 represents a significant increase in Mg content, which strongly indicates the presence of Mg rods at those specific locations. The sharp and distinct peaks in

Mg intensity serve as clear markers, signifying the precise positions where the Mg rods were welded into the sample during the WAAM process.

A distinct density of Mg compared to aluminum introduces the possibility of intrinsic mechanical defects during the fusion of Mg rods into the aluminum sample. As Mg inclusions are integrated into the material, the dissimilar densities of Mg and aluminum can create stress concentrations and potential voids, compromising the sample's structural integrity and mechanical properties. Besides, Mg inclusions manifest a strong porosity (these are dark dots in the area which circled in red) as seen from a CT picture of those areas shown in Fig. 22.

a)

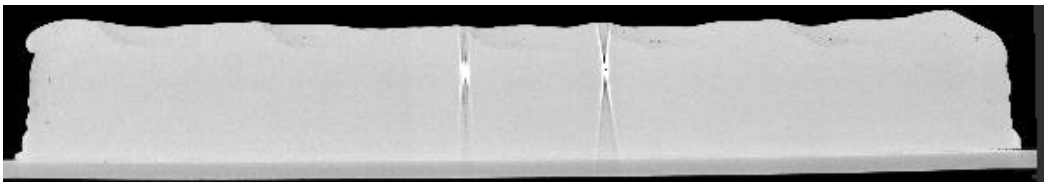

b)

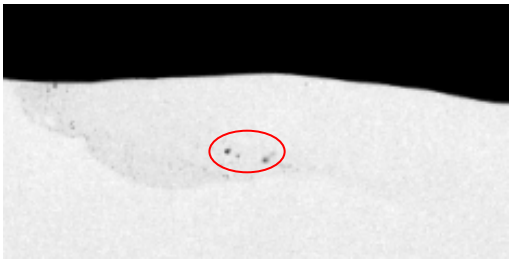

Figure 22 a,b: CT pictures of the sample with Mg inclusions (a), zoomed in picture of the Mg part (b).

As a result, the chemical defects in the specimen are the sources of ultrasound scattering, i.e. become mechanical defects and also must be recognized by the LUS scan. This is clearly seen from Fig. 23, a where the LUS B-scan of the specimen is shown. The noisy areas in Fig. 23 are caused by porosity in Mg inclusions which are identified by LUS along with real mechanical defects (drilled holes in red on the figure) (Fig. 23). Overlap of LIBS results (Fig. 24) with LUS B-scan and CT show that that both techniques (LIBS and LUS) locate correct positions of Mg rods and can identify the presence of the inclusions with ease. In Figure 24, a slight displacement is noticeable among the techniques, attributed to variations in the data points for each experiment. This displacement indicates a high level of accuracy in the comparison but falls short of being absolutely perfect. Nonetheless, Figure 24

provides evidence that the combined use of LIBS and LUS is effective in accurately determining the accurate placements of Mg rods and detecting the presence of inclusions.

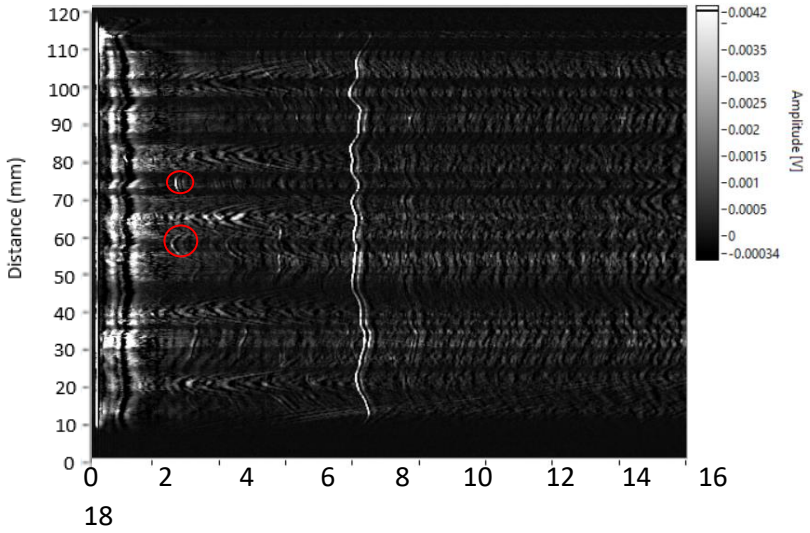

Figure 23. LUS B-scan of the specimen with Mg inclusions.

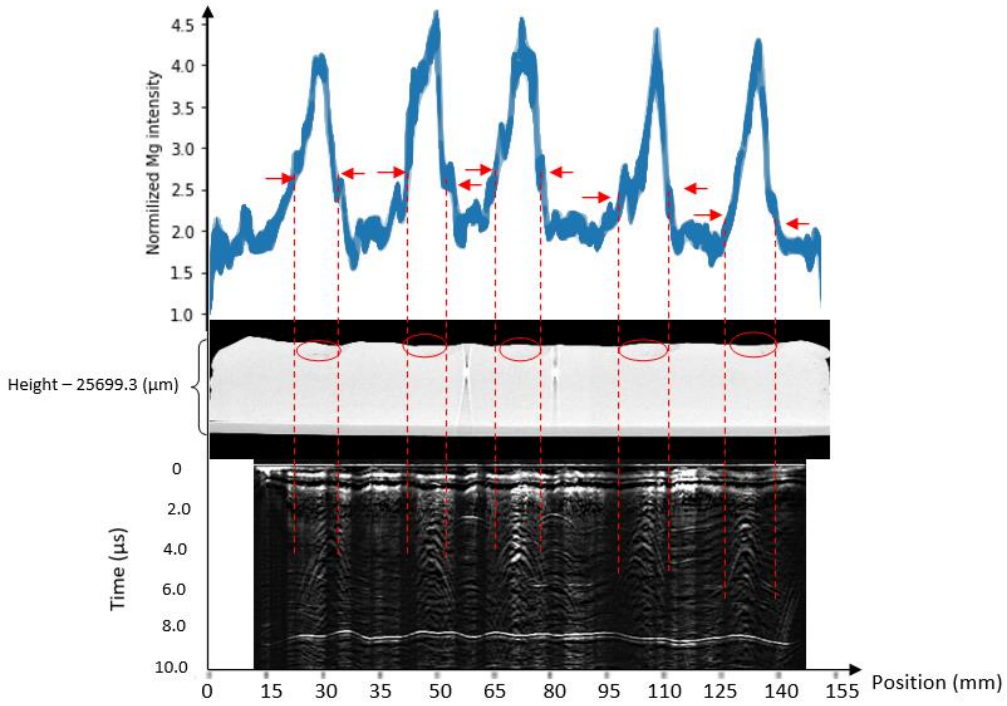

Figure 24. LUS B-scan of the specimen with Mg inclusions overlapped with LIBS results (Fig. 21).

On the other hand, the interference caused by the Mg inclusions in the LUS B-scans may present challenges in accurately characterizing the material and identifying potential defects. This is where the complementary nature of the LIBS method came to the forefront: LIBS analysis takes care of the chemical inclusions while LUS visualizes mechanical inhomogeneities.

Thus, the combination of LUS and LIBS in this study proved to be highly complementary, enabling a comprehensive evaluation of the aluminum sample with Mg inclusions. The synergy between these two NDT methods allows to gain a deeper understanding of the inner structure of the material. LUS ability to detect and locate mechanical defects further supported and validated the LIBS results, which confirmed the presence of Mg inclusions at the locations corresponding to the observed noisy areas in the B-scan.

Conclusions

Additive manufacturing of metallic components using WAAM is accompanying by high temperature impact on a material which results in both variation in its chemical composition and initiation of mechanical defects. That changes the character of NDT for WAAM parts with mandatory involvement of both analysis of the material chemical elemental structure and the defects produced. This study has evaluated the applicability of LIBS and LUS as complementary approaches to the above NDT constituents and has brought about the following conclusions:

LUS

- Single-sided LUS B-Scan in the reflection mode of the WAAM substrate evaluates the distribution of bonding strength along the contact line with AM specimen
- LUS C-scan enables to visualize 2D-contact area between the AM specimen and the substrate which is shown to replicate an optically scanned image of this plane
- LUS has demonstrated a high sensitivity and resolution in detecting and 100% accuracy in locating both artificial and naturally produced defects: $\approx$1mm drilled holes, mm-size bubbles and interlayer bonding within the specimen
- As a complementary technique LUS also identifies chemical inclusions (due to the higher porosity and density of Mg in Al) and locates mechanical defects (holes) in metallic specimen.

LIBS

- The Python code developed and applied for LIBS analysis enables to visualize and process LIBS data (code can choose the line of the element that should be examined, normalize it, track the intensity change of the line through the whole experiment and plot it)
- In the presence of a calibration specimen, LIBS is shown to precisely evaluate the absolute values in the gradient of Si component closely agreed with spark spectroscopy results
- LIBS demonstrated reliable detection within % accuracy in determining chemical inclusions (Mg) in WAAM AL specimens
- LIBS B-Scan reliably reproduces the distribution of chemical impurities (Mg) in Al specimens containing both chemical and mechanical inhomogeneities.

References

[1] Schnars, U., et al. Applications of NDT methods on composite structures in aerospace industry. In Proceedings of the Conference on Damage in Composite Materials, Stuttgart, Germany: (2006, September), 18-19

[2] Misokefalou, D., et al. Non-destructive testing for quality control in automotive industry. Int. J. Eng. Appl. Sci. Technol: (2022), 7, 349-355.

[3] Gupta, M., et al. Advances in applications of Non-Destructive Testing (NDT): A review. Advances in Materials and Processing Technologies: (2022), 8(2), 2286-2307.

[4] Newton, K., et al. NDT research for the oil and gas industry. British Journal of Non-Destructive Testing: (1992), 34(3).

[5] Márquez, F. P. G., & et al. A review of non-destructive testing on wind turbines blades. Renewable Energy: (2020), 161, 998-1010.

[6] Dilberoglu, U. M., et al. The role of additive manufacturing in the era of industry 4.0. Procedia manufacturing: (2017), 11, 545-554.

[7] Shaloo, M., et al. A review of Non-Destructive Testing (NDT) techniques for defect detection: application to fusion welding and future wire arc additive manufacturing processes. Materials: (2022), 15(10), 3697.

[8] Honarvar, F., et al. A review of ultrasonic testing applications in additive manufacturing: Defect evaluation, material characterization, and process control. Ultrasonics: (2020), 108, 106227.

[9] An, Y-K., et al. Piezoelectric transducers for assessing and monitoring civil infrastructures. Sensor technologies for civil infrastructures. Woodhead Publishing: 2014. 86-120.

[10] Serrati, Douglas SM, et al. Non-Destructive Testing inspection for metal components produced using wire and arc additive manufacturing. Metals: (2023), 13.4, 648.

[11] Li, J., et al. Spatially selective excitation in laser-induced breakdown spectroscopy combined with laser-induced fluorescence. Optics Express: (2017), 25(5), 4945-4951.

[12] Li, J., et al. Evaluation of the self-absorption reduction of minor elements in laser-induced breakdown spectroscopy assisted with laser-stimulated absorption. Journal of Analytical Atomic Spectrometry: (2017), 32(11), 2189-2193.

[13] Tang, Y., et al. Multi-elemental self-absorption reduction in laser-induced breakdown spectroscopy by using microwave-assisted excitation. Optics Express: (2018), 26(9), 12121-12130.

[14] Li, T., et al. Correction of self-absorption effect in calibration-free laser-induced breakdown spectroscopy (CF-LIBS) with blackbody radiation reference. Analytica Chimica Acta: (2019), 1058, 39-47

[15] Hou, J., et al. Development and performance evaluation of self-absorption-free laser-induced breakdown spectroscopy for directly capturing optically thin spectral line and realizing accurate chemical composition measurements. Optics express: (2017), 25(19), 23024-23034.
[16] Yi, R., et al. Investigation of the self-absorption effect using spatially resolved laser-induced breakdown spectroscopy. Journal of Analytical Atomic Spectrometry: (2016), 31(4), 961-967.
[17] Hoffmann, A., et al. Calculation and measurement of the ultrasonic signals generated by ablating material with a Q-switched pulse laser. Applied surface science: (1996), 96, 71-75.
[18] Hoffmann, A., et al. Modeling of the ablation source in laser-ultrasonics. In AIP Conference Proceedings: American Institute of Physics, (2000, May), Vol. 509, No. 1, 279-286.
[19] Moon, H. Y., et al. On the usefulness of a duplicating mirror to evaluate self-absorption effects in laser induced breakdown spectroscopy. Spectrochimica Acta Part B: Atomic Spectroscopy: (2009), 64(7), 702-713.
[20] Murray, T. W., et al. Thermoelastic and ablative generation of ultrasound: source effects. Review of Progress in Quantitative Nondestructive Evaluation: (1998), Volume 17A, 619-625.
[22] Rose, L. R. F. Point-source representation for laser-generated ultrasound. The Journal of the Acoustical Society of America: (1984), 75(3), 723-732.
[22] Spicer, J. B. Laser Ultrasonics in Finite Structures: Comprehensive Modelling with Supporting Experiment: (1991), Ph. D. Thesis.
[23] McDonald, F. A. Practical quantitative theory of photoacoustic pulse generation. Applied Physics Letters: (1989), 54(16), 1504-1506.
[24] Cheng, J. C., et al. Excitations of thermoelastic waves in plates by a pulsed laser. Applied Physics: (1995), A, 61, 311-319.
[25] Dewhurst, R. J., et al. Quantitative measurements of laser-generated acoustic waveforms. Journal of Applied Physics: (1982), 53(6), 4064-4071.
[26] Monchalin, J. P. Laser-ultrasonics: Principles and industrial applications. In Ultrasonic and advanced methods for nondestructive testing and material characterization: (2007), 79-115.
[27] Hutchins, D. A. Ultrasonic generation by pulsed lasers. In Physical acoustics: (1988), Vol. 18, 21-123. Academic Press.
[28] Scruby, C.B.; Drain, L.E. Laser Ultrasonics: Techniques and Applications; Routledge: (2019), England, UK,; ISBN 9780203749098
[29] Djordjevic, B. B., et al. Guided wave non-contact ultrasonic for NDE. 16th World Conference on NDT: (2004), Montreal, Canada.
[30] Williams, S. W., et al. Wire Arc Additive Manufacturing. Mater. Sci. Technol. 2016, 32, 641–647.

[31] Wu, B. A review of the wire arc additive manufacturing of metals: properties, defects and quality improvement. Journal of manufacturing processes: (2018), 35, 127-139.
[32] Lednev, V. N., et al. Laser induced breakdown spectroscopy for in-situ multielemental analysis during additive manufacturing process. In Journal of Physics: IOP Publishing, Conference Series (2018, November), Vol. 1109, No. 1, 012050.
[33] Taparli, U. A. In situ laser-induced breakdown spectroscopy measurements of chemical compositions in stainless steels during tungsten inert gas welding. Spectrochimica Acta Part B: Atomic Spectroscopy: (2018), 139, 50-56.
[34] Shah, S. K. H. Laser induced breakdown spectroscopy methods and applications: A comprehensive review. Radiation physics and chemistry: (2020), 170, 108666.
[35] Blouin, A. et al. Improved resolution and signal-to-noise ratio in laser-ultrasonics by SAFT processing. Optics Express: (1998), 2(13), 531-539.
[36] Klein, M.B., et al. Signal processing methods for non-destructive evaluation using ultrasonics. NDT&E Int: (1998), 31, 93–97
[37] Zeng, Y. Laser Ultrasonic inspection of a Wire+ Arc Additive Manufactured (WAAM) sample with artificial defects. Ultrasonics: (2021), 110, 106273.
[38] Lévesque, D. Inspection of additive manufactured parts using laser ultrasonics. In AIP Conference Proceedings: AIP Publishing, (2016, February), Vol. 1706, No. 1, 130003-1 – 130003-8.
[39] Ma, Yuyang, et al. Laser opto-ultrasonic dual detection for simultaneous compositional, structural, and stress analyses for wire+ arc additive manufacturing. Additive Manufacturing: (2020), 31, 100956.
[40] Wu, B., et al. A review of the wire arc additive manufacturing of metals: properties, defects and quality improvement. Journal of manufacturing processes: (2018), 35, 127-139.
[41] NIST LIBS Database (https://physics.nist.gov/PhysRefData/ASD/LIBS/libs-form.html)
[42] Lovshenko, F. G. Mechanicheskoe legirovanie aluminievykh materialov s osobymi fiziko-mechanicheskimi svoistvami: (2001), (in Russian), 76-82.